Exclusive $\pi^+\pi^-$ Electroproduction
HERMES/NIKHEF Group Meeting
11 December 2003

Keith Griffioen
NIKHEF and College of William and Mary

December 12, 2003

Abstract

I have reproduced Riccardo Fabbri's analysis of exclusive $\pi^+\pi^-$ production in HERMES, and have written a toy Monte Carlo simulation to study the effect of acceptance on the determination of Legendre moments.

Exclusive 2-Pion Production

HERMES/NIKHEF Group Meeting 11 Dec 03
Keith Griffioen

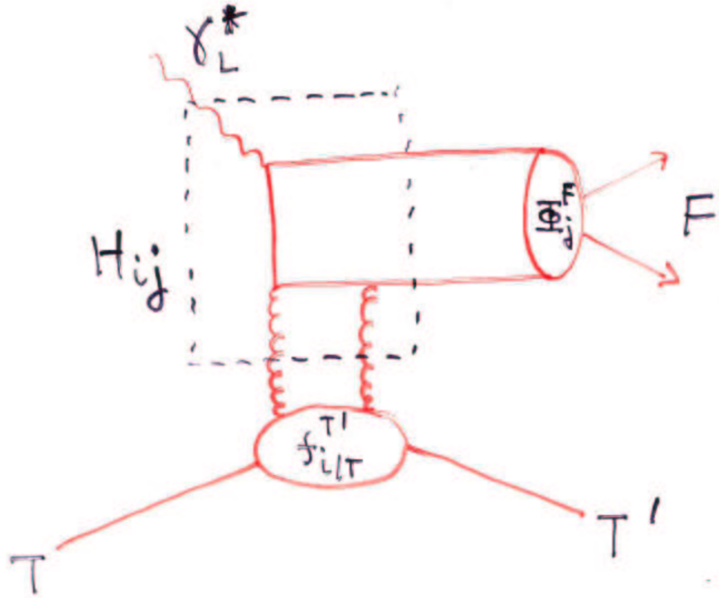

$$\mathcal{M} = \sum_{ij} \int dz\, dx_1 \underbrace{f^{T'}_{i/T}(x_1, x_1 - x_{Bj}, t)}_{\text{GPD}} \underbrace{H_{ij}\left(\frac{x_1}{x_{Bj}}, Q^2, z\right)}_{\text{pQCD}} \underbrace{\Phi^F_j(z)}_{\substack{\text{distribution amplitude} \\ \text{for hadronic state F}}}$$

$+\mathcal{O}\left(\frac{1}{Q}\right)$ corrections

Factorization Theorem Collins, Frankfurt, Strikman PRD 56 (97) 2982.

no proven factorization thrm for γ^*_T (transverse photons) but amplitudes are down by $1/Q$ w.r.t. γ^*_L

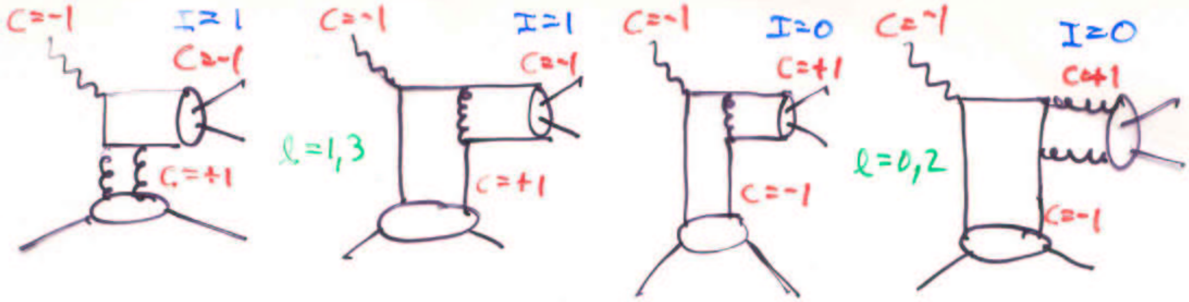

ρ-like

$\rho(770)$ $I^G(J^{PC}) = 1^+(1^{--})$

f-like

$f_0(980)$ $0^+(0^{++})$

$f_2(1270)$ $0^+(2^{++})$

Charge Conjugation $\quad \mathcal{U}_c|A=0\rangle = \eta_c|A=0\rangle \quad \boxed{\eta_c = \pm 1}$

A = additive Q#'s $\quad Q, I_3, B, L, Y$

photons: $\quad j_\mu^{em} \xrightarrow{\mathcal{U}_c} -j_\mu^{em}$ (charge reverses)

$\Box^2 A_\mu = j_\mu^{em} \quad \therefore \quad A_\mu \xrightarrow{\mathcal{U}_c} -A_\mu \quad \boxed{\eta_c = -1 \text{ for } \gamma}$

and gluon!

2γ or $2g$ has $\eta_c = 1$

$\therefore \pi^0 \to 2\gamma \Rightarrow \eta_c^{\pi^0} = +1$

$q\bar{q}$: total w.f. antisymmetric

reverse particles: $\begin{cases} \text{spatial exchange} & (-1)^\ell \\ \text{spin exchange} & (-1)^{S+1} \\ \text{charge exchange} & \eta_c \end{cases}$ $\quad$ triplet S, singlet A

$\eta_c(-1)^{\ell+S+1} = -1 \quad \boxed{\eta_c = (-1)^{\ell+S}}$

$\pi^+\pi^-$: symmetric w.f. $\Rightarrow \eta_c(-1)^\ell = 1$ (no spin)

isospin:

$|I=1, I_3=1\rangle = \frac{1}{\sqrt{2}}(\pi^+\pi^0 - \pi^0\pi^+)$

$|I=1, I_3=0\rangle = \frac{1}{\sqrt{2}}(\pi^+\pi^- - \pi^-\pi^+)$

$|I=1, I_3=-1\rangle = \frac{1}{\sqrt{2}}(\pi^0\pi^- - \pi^-\pi^0)$

antisym.

$|I=0, I_3=0\rangle = \frac{1}{\sqrt{3}}(\pi^+\pi^- - \pi^0\pi^0 + \pi^-\pi^+)$

sym.

odd $\ell \Rightarrow I=1 \qquad$ even $\ell \Rightarrow I=0$

B. Lehmann-Dronke et. al PLB 475 (00) 147
PRD 63 (01) 114001

Exclusive $\pi\pi$

$$T^{\pi^+\pi^-} = T^{I=0} + T^{I=1}$$
$$T^{\pi^0\pi^0} = T^{I=0}$$
$$T^{I=0} \propto \Phi^{I=0} \{\text{integrated GPDs}\}$$
$$T^{I=1} \propto \Phi^{I=1} \{\text{integrated GPDs}\}$$

$$\Phi^{I=0} \propto f_0(m_{\pi\pi}) P_0(\cos\theta) + c\, f_2(m_{\pi\pi}) P_2(\cos\theta)$$
$$\Phi^{I=1} \propto F_\pi(m_{\pi\pi}) P_1(\cos\theta)$$

$$\sigma \propto |T^{\pi^+\pi^-}|^2 = b_{00} P_0^2 + b_{01} P_0 P_1 + b_{02} P_0 P_2 + b_{11} P_1^2 + b_{12} P_1 P_2 + b_{22} P_2^2$$

$$\langle P_\ell \rangle = \frac{\int \sigma P_\ell\, dx}{\int \sigma\, dx} \qquad x \equiv \cos\theta$$

$$\boxed{\langle P_1 \rangle = \frac{\frac{2}{3} b_{01} + \frac{4}{15} b_{12}}{b_{00} + b_{11} + b_{22}}}$$

$$\boxed{\langle P_3 \rangle = \frac{\frac{6}{35} b_{12}}{b_{00} + b_{11} + b_{22}}}$$

$$b_{01} \propto f_0(m_{\pi\pi}) F_\pi(m_{\pi\pi})$$
$$b_{12} \propto \underbrace{f_2(m_{\pi\pi})}_{\text{Omnès functions}} \underbrace{F_\pi(m_{\pi\pi})}_{\pi \text{ form factor}}$$

$$\langle P_1 \rangle - \frac{14}{9} \langle P_3 \rangle = \frac{\frac{2}{3} b_{01}}{b_{00} + b_{11} + b_{22}}$$

$$f_\ell(m_{\pi\pi}) = \exp\left[i\, \underbrace{\delta_\ell^0(m_{\pi\pi})}_{\pi\pi \text{ phase shifts}} + \frac{m_{\pi\pi}^2}{\pi} \mathrm{Re} \int_{4m_\pi^2}^{\infty} ds\, \frac{\delta_\ell^0(s)}{s(s - m_{\pi\pi}^2 - i0)} \right]$$

Formalism is only for γ_L^* & in 1st order

In general $\sigma = \sum_{\substack{JJ' \\ \lambda\lambda'}} \rho_{\lambda\lambda'}^{JJ'} Y_{J\lambda}(\theta,\phi) Y_{J'\lambda'}(\theta,\phi)$

Re-express as $\sigma = \sum_{LM} a_{LM} Y_{LM}(\theta,\phi)$

$$a_{10} = \frac{1}{\sqrt{4\pi}} \left\{ 4\sqrt{\tfrac{3}{5}}\, \rho_{11}^{21} + 4\sqrt{\tfrac{1}{5}}\, \rho_{00}^{21} + 2\rho_{00}^{10} \right\}$$

$$a_{30} = \frac{1}{\sqrt{4\pi}} \left\{ -12\sqrt{\tfrac{1}{35}}\, \rho_{11}^{21} + 6\sqrt{\tfrac{3}{35}}\, \rho_{00}^{21} \right\}$$

Then, $\langle P_1 \rangle = \sqrt{\frac{4\pi}{3}}\, a_{10}$

$\langle P_3 \rangle = \sqrt{\frac{4\pi}{7}}\, a_{30}$

- γ_L^* has 0 helicity
- s-channel helicity conservation $\Rightarrow \pi^+\pi^-$ has 0 helicity
- only ρ_{00} states populated by γ_L^*

$$\boxed{\langle P_1 \rangle + \frac{7}{3}\langle P_3 \rangle = \frac{4+2\sqrt{3}}{\sqrt{15}}\, \rho_{00}^{21} + \frac{2}{\sqrt{3}}\, \rho_{00}^{10}}$$

Legendre Polynomials

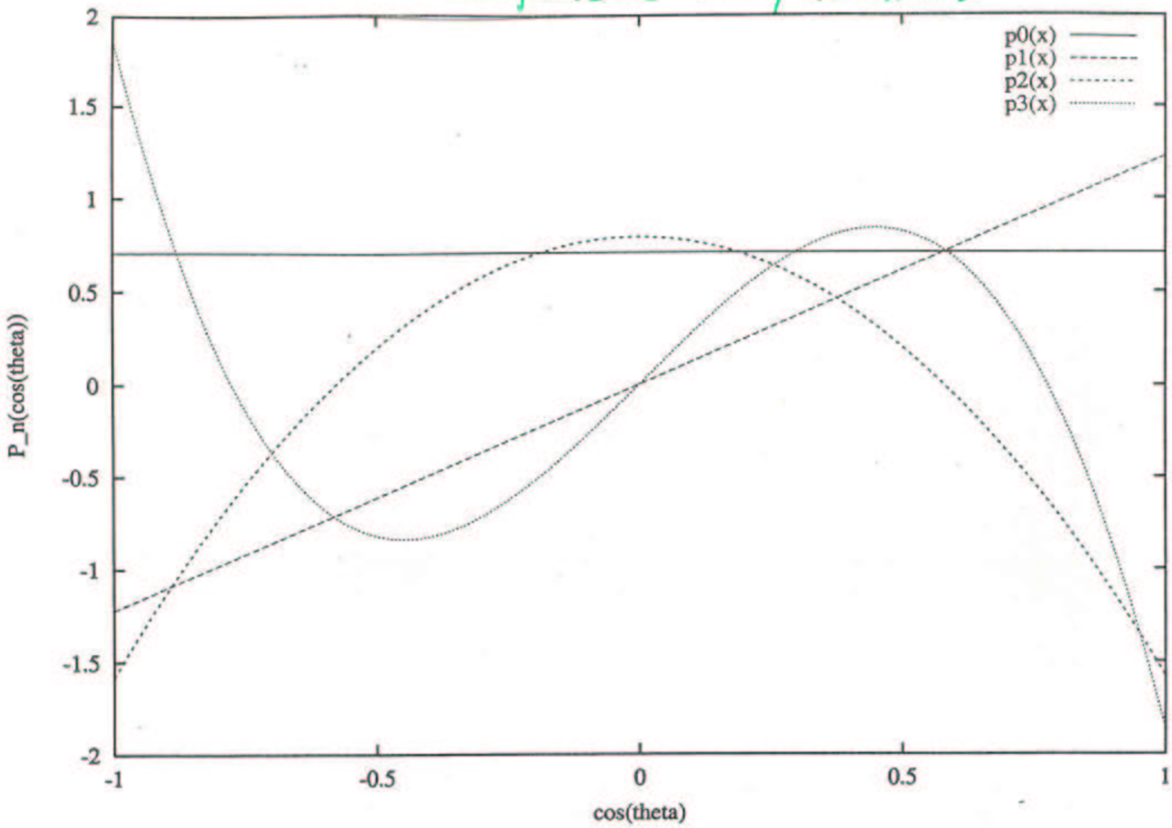

$$\frac{d\sigma^{\pi^+\pi^-}}{d\cos\theta} = \sum_{\ell\ell'} a_{\ell\ell'} P_\ell(\cos\theta) P_{\ell'}(\cos\theta)$$

$$P_0(x) = 1$$

$$P_1(x) = x$$

$$P_2(x) = \frac{1}{2}(3x^2-1)$$

$$P_3(x) = \frac{1}{2}(5x^3-3x)$$

Lehmann-Dronke

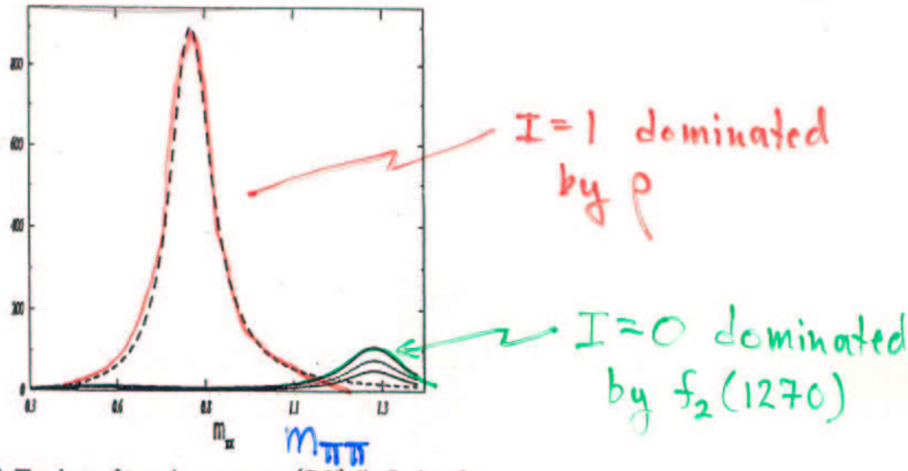

Fig. 2. The shape of two-pion mass $m_{\pi\pi}$ (GeV) distributions for pions with isospin one (dashed curve) and isospin zero (solid curves). The isospin zero distributions are plotted for Bjorken $x = 0.3, 0.4, 0.5$. (The larger x_{Bj} the more enhanced is the distribution.)

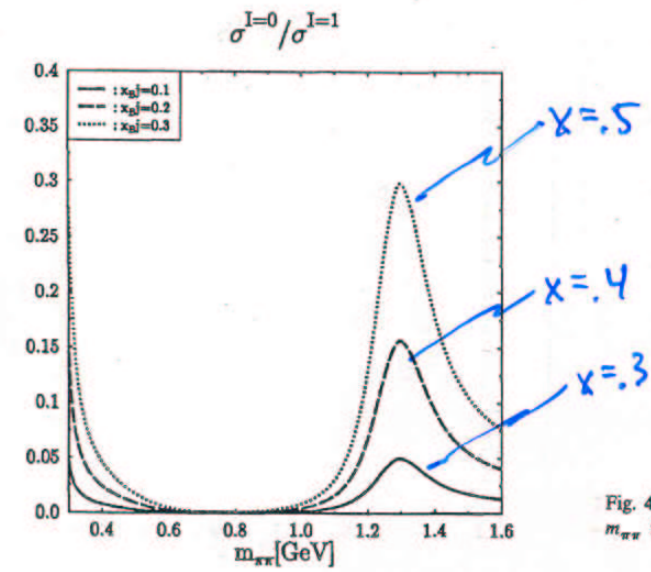

FIG. 3. The ratio of the differential cross sections for isoscalar and isovector pion pair production at three different values for x_{Bj} as a function of $m_{\pi\pi}$.

$m_{\pi\pi}$

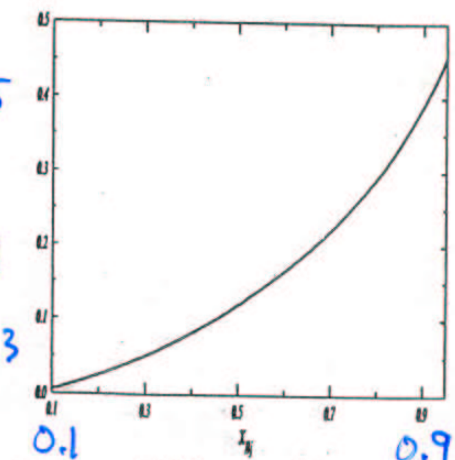

Fig. 4. The ratio of $\frac{d\sigma^{\pi^0\pi^0}}{dt}|_{t=t_{min}}$ to $\frac{d\sigma^{\pi^+\pi^-}}{dt}|_{t=t_{min}}$ integrated over $m_{\pi\pi}$ from the threshold to 1.4 GeV as a function of Bjorken x.

x_{Bj}

for $\frac{\sigma(I=0) \text{ at } t_{min}}{\sigma(I=1,0) \text{ at } t_{min}}$

Lehmann-Dronke

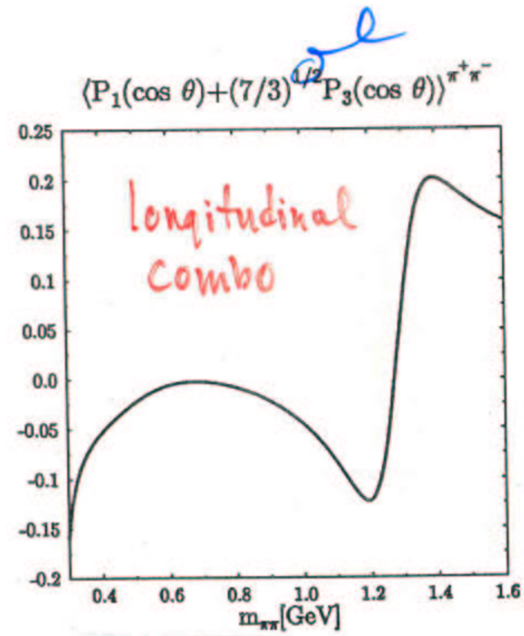

FIG. 6. $\langle P_1(\cos\theta)\rangle^{\pi^+\pi^-} + \sqrt{\frac{7}{3}}\,\langle P_3(\cos\theta)\rangle^{\pi^+\pi^-}$ as a function of $m_{\pi\pi}$ with cross sections integrated over $x_{\rm Bj}$ from 0.05 to 0.4.

$m_{\pi\pi}$

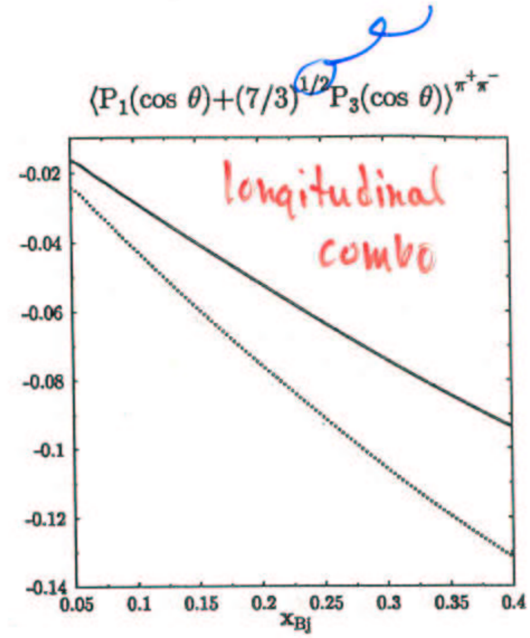

FIG. 7. $\langle P_1(\cos\theta)\rangle^{\pi^+\pi^-} + \sqrt{\frac{7}{3}}\,\langle P_3(\cos\theta)\rangle^{\pi^+\pi^-}$ as a function of $x_{\rm Bj}$ with cross sections integrated over $m_{\pi\pi}$ from the threshold to 0.6 GeV. The dotted line shows the corresponding result obtained using the fit of [26] instead of the Padé approximation for the Omnès function $f_0(m_{\pi\pi})$.

x_{Bj}

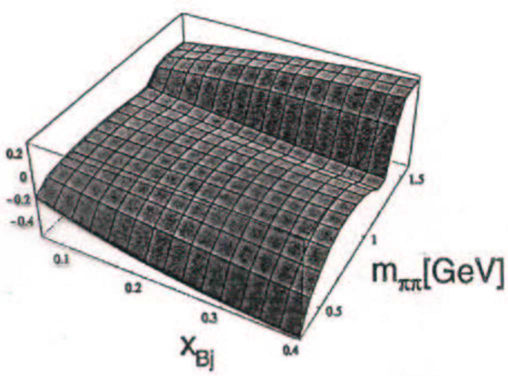

FIG. 4. $\langle P_1(\cos\theta)\rangle^{\pi^+\pi^-}$ as a function of $x_{\rm Bj}$ and $m_{\pi\pi}$.

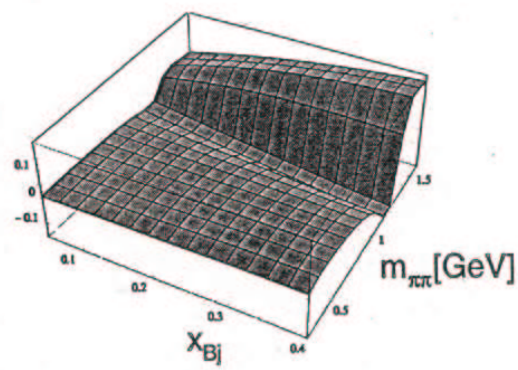

FIG. 5. $\langle P_3(\cos\theta)\rangle^{\pi^+\pi^-}$ as a function of $x_{\rm Bj}$ and $m_{\pi\pi}$.

$\underbrace{\text{2-d}}$ plots of moments $\langle P_\ell \rangle$

$(x_{Bj}, m_{\pi\pi})$

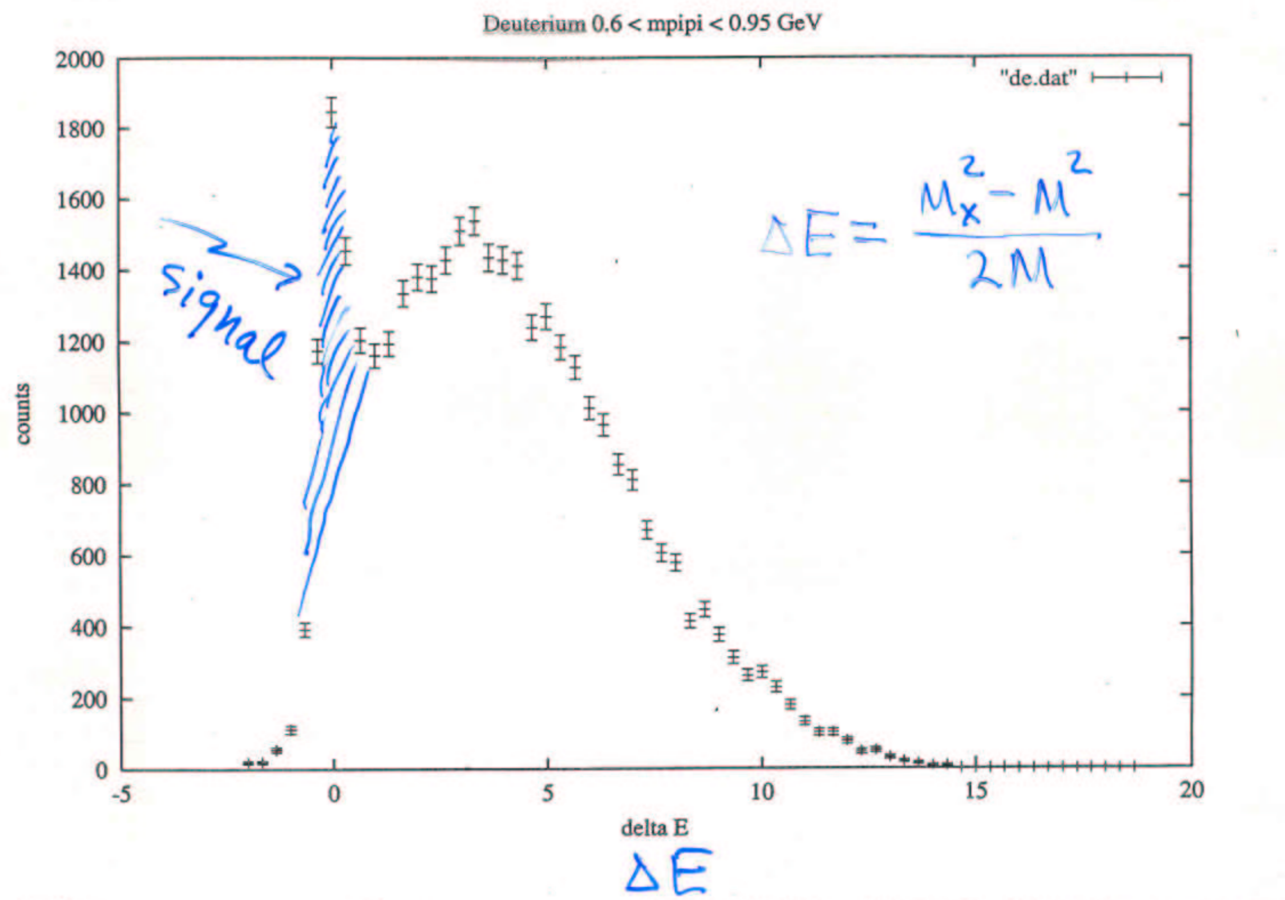
Deuterium 0.6 < mpipi < 0.95 GeV
"de.dat"
counts
delta E
signal
$\Delta E = \frac{M_x^2 - M^2}{2M}$
ΔE

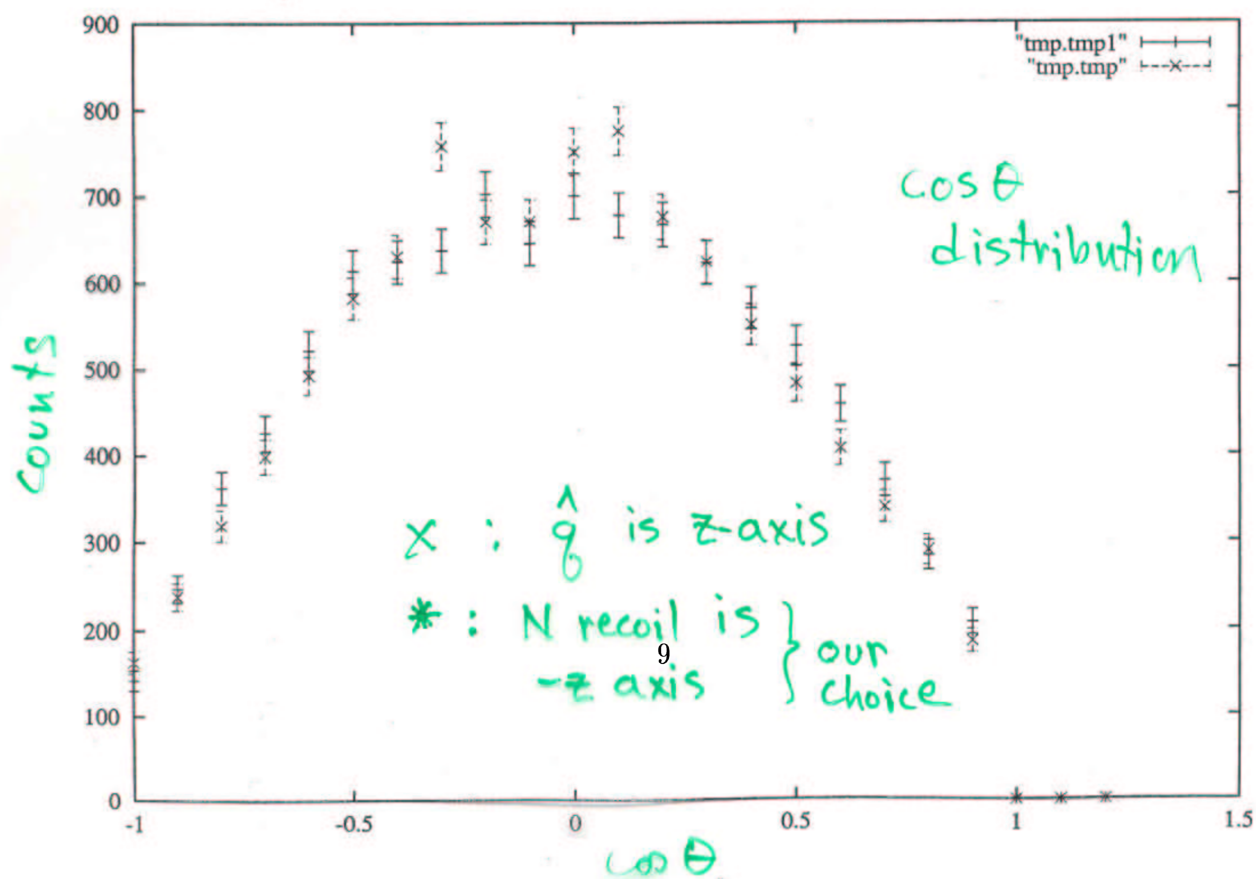
"tmp.tmp1"
"tmp.tmp"
cos θ distribution
counts
x : $\hat{q}$ is z-axis
* : N recoil is -z axis } our choice
cos θ

Riccardo Fabri's paper (now circulating in HERMES)

I=0 ℓ=2

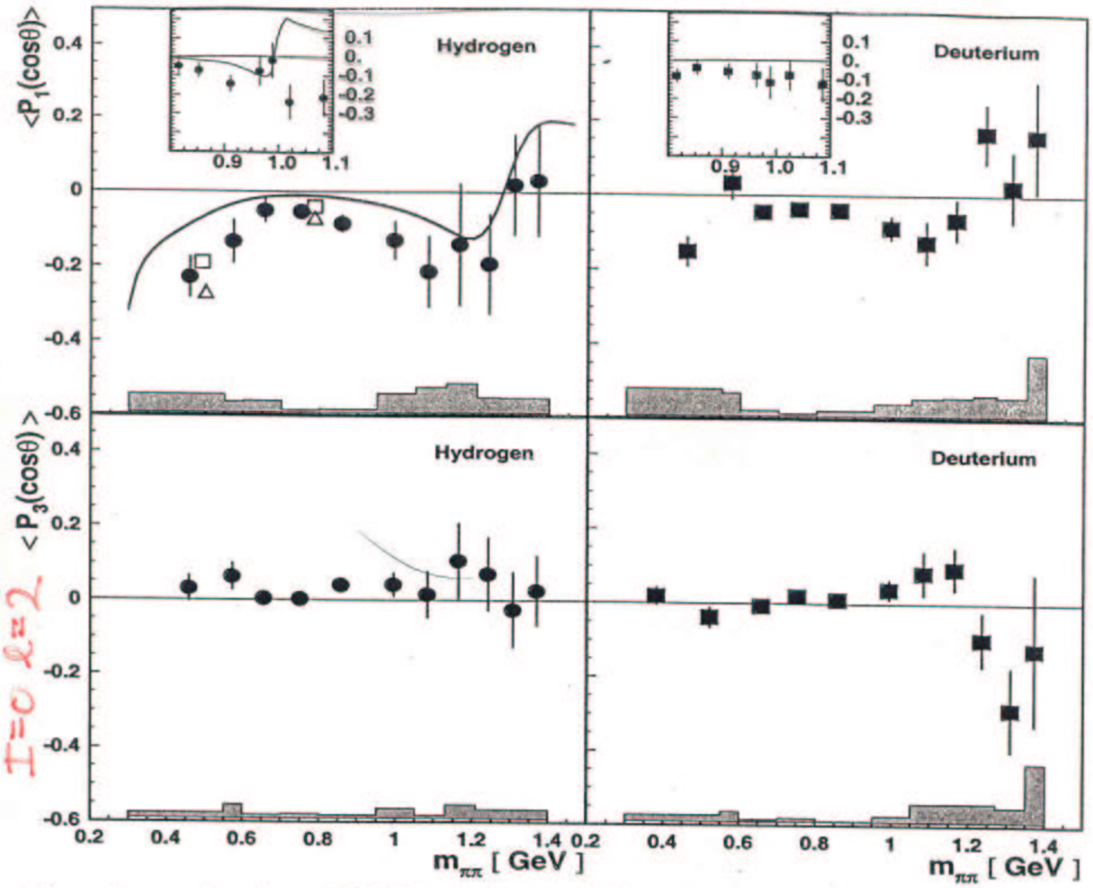

Figure 4. $m_{\pi\pi}$-dependence of the *intensity densities* $\langle P_1(\cos\theta)\rangle$, upper panels, and $\langle P_3(\cos\theta)\rangle$, bottom panels, for both hydrogen and deuterium, left and right panels respectively. In the upper panels, the region $0.8 < m_{\pi\pi} < 1.1$ GeV rebinned in finer channels to better investigate possible contributions from the narrow $f_0(980)$ meson resonance. Also shown are leading twist predictions for the hydrogen target including the two-gluon exchange mechanism contribution, LSPG [4,5] (solid curve at $x = 0.16$). A calculation without the gluon exchange contribution is showed for limited $m_{\pi\pi}$ values, LPPSG [6] (open squares at $x = 0.1$, open triangles at $x = 0.2$). Fig. 1-a. In the above predictions, the contribution from f_0 meson decay was not considered. Instead, in the zoomed panel for the hydrogen target, the prediction from [18], which includes the f_0 meson contribution, is shown. All experimental data have $< x >= 0.16$ and $< Q^2 > = 3$ GeV^2. The systematic uncertainty is represented by error band.

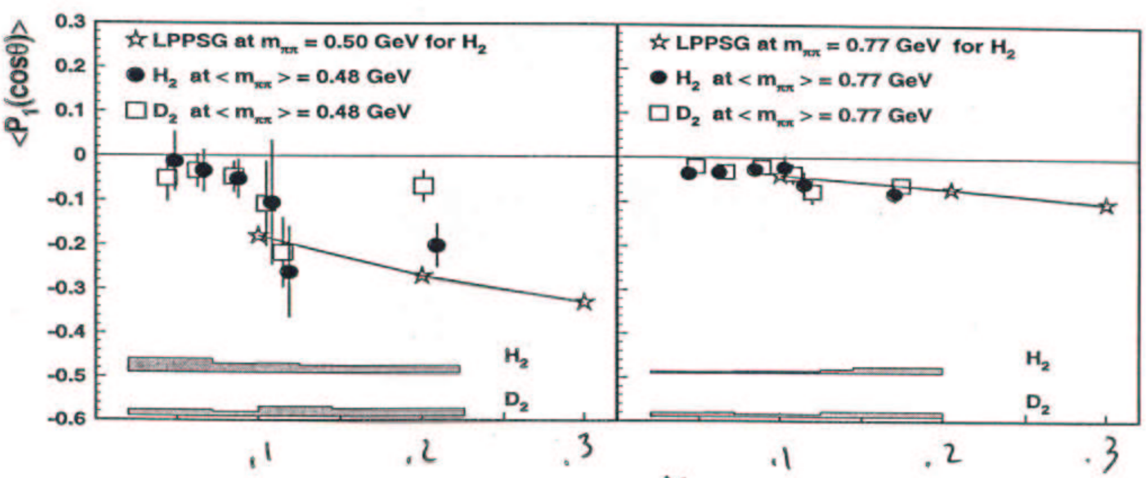

X

Figure 6. The x-dependence of the *intensity densities* $\langle P_1(\cos\theta)\rangle$ for both targets separately, in the regions $0.30 < m_{\pi\pi} < 0.60$ GeV (left panels) and $0.60 < m_{\pi\pi} < 0.95$ GeV (right panels). Theoretical predictions from LPPSG [6] (stars) for hydrogen are compared with the data. In these computations, the two-gluon exchange mechanism contribution to the process is neglected. The systematic uncertainty is given by the error band.

Riccardo's
Combinations

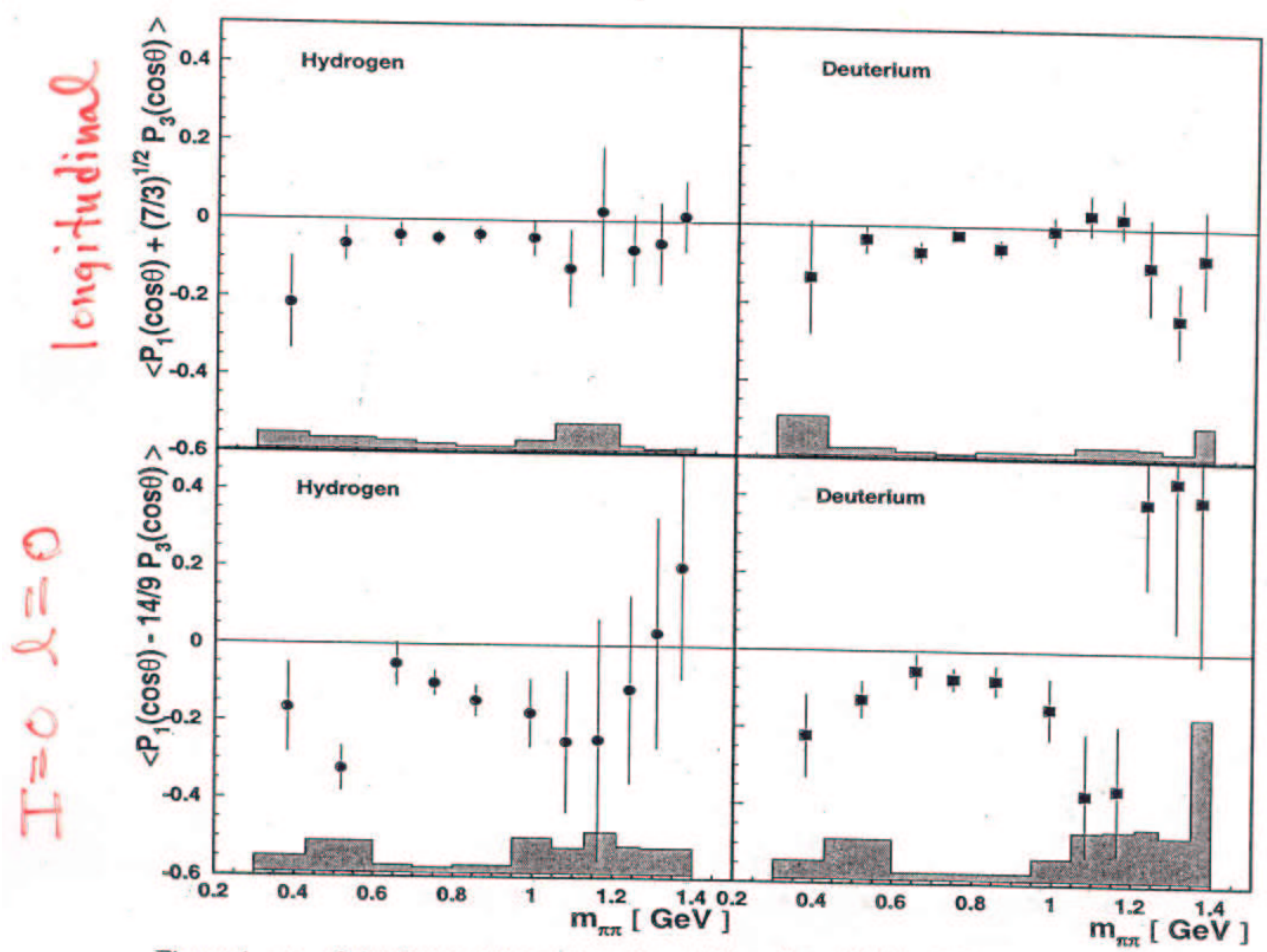

Figure 4. $m_{\pi\pi}$-dependence of the combinations $\langle P_1(cos\theta) + \sqrt{(7/3)} \cdot P_3(cos\theta)\rangle$, upper panels, and $\langle P_1(cos\theta) - 14/9 \cdot P_3(cos\theta)\rangle$, bottom panels, for both hydrogen and deuterium targets, left and right panels respectively. All experimental data have $< x >= 0.16$ and $< Q^2 > = 3$ GeV^2. The systematic uncertainty is given as error bands.

Experimental Moments
$\langle P_\ell \rangle$

$$\langle P_\ell \rangle = \frac{\int P_\ell(x)\,\sigma(x)\,dx}{\int \sigma(x)\,dx} \qquad x \equiv \cos\theta$$

Method 1: make histogram; numerically integrate

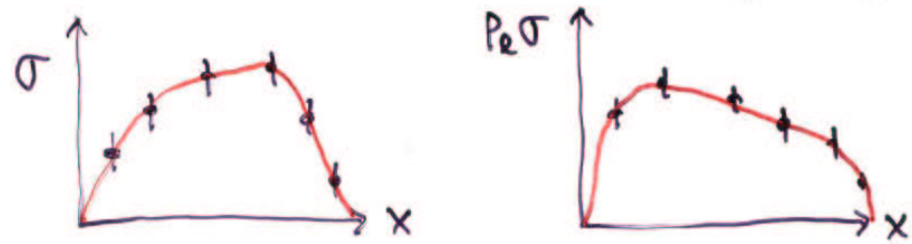

Method 2:

$$\boxed{\langle P_\ell \rangle = \frac{1}{N} \sum_j P_\ell(\cos\theta_j)}$$

proof: numerical integration $\displaystyle \langle P_\ell \rangle = \frac{\sum_j P_\ell(x_j)\, N_j\, \Delta X}{\sum_j N_j\, \Delta X}$

$N_j \equiv$ # of counts in bin j

$$\langle P_\ell \rangle = \frac{1}{N} \underbrace{\sum_j}_{\text{sum over bins}} P_\ell(x_j)\, N_j = \frac{1}{N} \underbrace{\sum_i}_{\text{sum over events}} P_\ell(x_i)$$

Error: Central limit Theorem (standard error of $\langle P_\ell \rangle$)

Variate $X \equiv \frac{1}{N} \sum_i x_i$ is normally distributed with $\mu_X = \mu_x$ and $\sigma_X = \sigma_x / \sqrt{N}$ for large N.

	advantage	disadvantage
method 1	Can correct spectrum with MC	requires good statistics
method 2	easy OK with limited statistics	can't correct for detector acceptance

Simple Monte Carlo

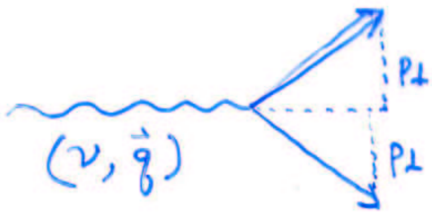

$$\left(\sqrt{m_{\pi\pi}^2 + p^2},\ \vec{p}_\perp,\ p_\parallel\right)$$

$\parallel$ along $\hat{q}$

$$\left(\sqrt{M^2 + r^2},\ -\vec{p}_\perp,\ r_\parallel\right)$$

input $\boxed{x,\ Q^2,\ m_{\pi\pi},\ p_\perp}$

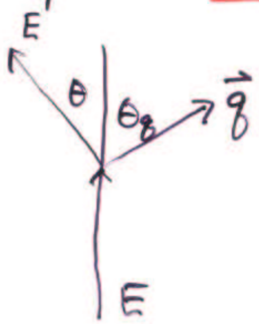

$\boxed{x, Q^2} \Rightarrow$ $\theta = 2 \operatorname{asin} \sqrt{Q^2/4EE'}$

$$q = \sqrt{E'^2 - 2EE'\cos\theta + E^2}$$

$$\theta_q = \operatorname{asin}(E' \sin\theta / q)$$

$$\boxed{\phi_q \ \text{random}\ [0, 2\pi]}$$

$$\boxed{q^\mu = (\nu,\ q\sin\theta_q\cos\phi_q,\ q\sin\theta_q\sin\phi_q,\ q\cos\theta_q)}$$

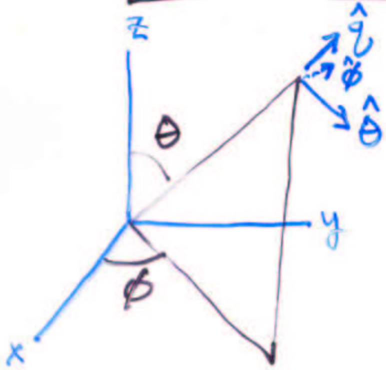

orthonormal vectors

$$\hat{q} = (\sin\theta_q\cos\phi_q,\ \sin\theta_q\sin\phi_q,\ \cos\theta_q)$$

$$\hat{\theta} = (\cos\theta_q\cos\phi_q,\ \cos\theta_q\sin\phi_q,\ -\sin\theta_q)$$

$$\hat{\phi} = (-\sin\phi_q,\ \cos\phi_q,\ 0)$$

$$\boxed{\phi_\perp \ \text{random}\ [0, 2\pi]}$$

$$\vec{p}_\perp = p_\perp(\cos\phi_\perp\,\hat{\theta}_q + \sin\phi_\perp\,\hat{\phi}_q)$$

$$\vec{p}_\parallel = p_\parallel\,\hat{q} \qquad \vec{r}_\parallel = r_\parallel\,\hat{q} \qquad \hat{p} = (\vec{p}_\parallel + \vec{p}_\perp)/p$$

$$r_\parallel + p_\parallel = q \qquad M + \nu = \sqrt{m_{\pi\pi}^2 + p^2} + \sqrt{M^2 + r^2}$$

MC

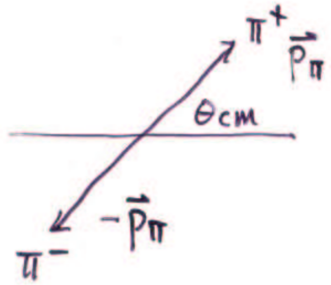

$$\boxed{p_\pi = \sqrt{\frac{m_{\pi\pi}^2}{4} - m_\pi^2}}$$

Lorentz Boost $\quad \gamma = \dfrac{\sqrt{m_{\pi\pi}^2 + p^2}}{m_{\pi\pi}}$

θ_{cm} chosen from specified distribution
ϕ_{cm} random $[0, 2\pi]$

$$\vec{p}_{\pm\parallel} = \gamma\left(\pm\, p_\pi \cos\theta_{cm} + \beta\sqrt{m_{\pi\pi}^2 + p_\pi^2}\right)\hat{p}$$

$$\vec{p}_{\pm\perp} = \pm\, p_\pi \sin\theta_{cm}\left[\cos\phi_{cm}\,\hat{\theta}_{cm} + \sin\phi_{cm}\,\hat{\phi}_{cm}\right]$$

unit vectors $\perp\ \hat{p}$

Acceptance

$$\theta_x^\pm = \mathrm{atan2}(p_x^\pm, p_z^\pm)$$
$$\theta_y^\pm = \mathrm{atan2}(p_y^\pm, p_z^\pm)$$

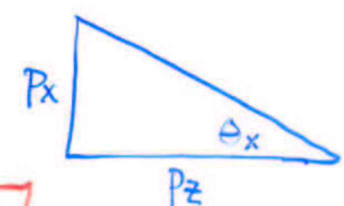

$p_\pm > 1$ GeV

$$-0.170 < \theta_x^\pm < 0.170$$
$$-0.140 < \theta_y^\pm < -0.040$$
$$0.040 < \theta_y^\pm < 0.140$$

$\Downarrow$ if true output $\cos\theta_{cm}$

Random Number Generation

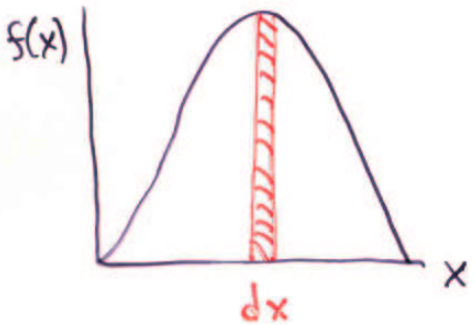

$f(x)\,dx$ is the probability of finding x in the interval dx.

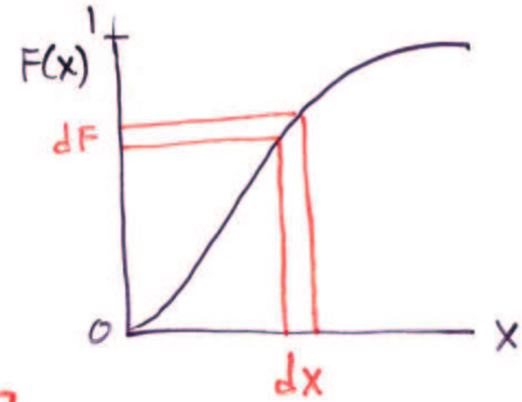

$$F(x) = \int_{-\infty}^{x} f(x)\,dx$$

$$\Rightarrow \frac{dF}{dx} = f(x)$$

$$\boxed{dF = f(x)\,dx}$$

picking F at random and calculating $x = F^{-1}(x)$ gives x with probability distribution $f(x)$

$f(x) = \frac{1}{2}(x+1)$ on $[-1,1]$

P_0, P_1

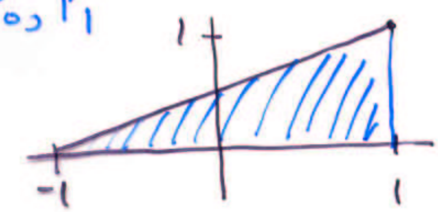

$$F(x) = \int_{-1}^{x} \frac{1}{2}(x+1)\,dx = \frac{1}{4}\left[x^2+2x+1\right]$$

$$\boxed{x = 2\sqrt{F} - 1}$$

$f(x) = \frac{1}{2}(1+x^3)$ on $[-1,1]$

P_0, P_1, P_3

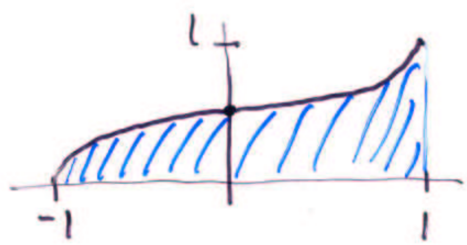

$$\boxed{x = 2\left(F - \tfrac{3}{8}\right) / \left(1 + \tfrac{x^3}{4}\right)}$$

iterate

Do isotropic CM distributions generate non-zero $\langle P_1 \rangle$ and $\langle P_3 \rangle$ due to holes in acceptance?

$\langle P_3 \rangle$

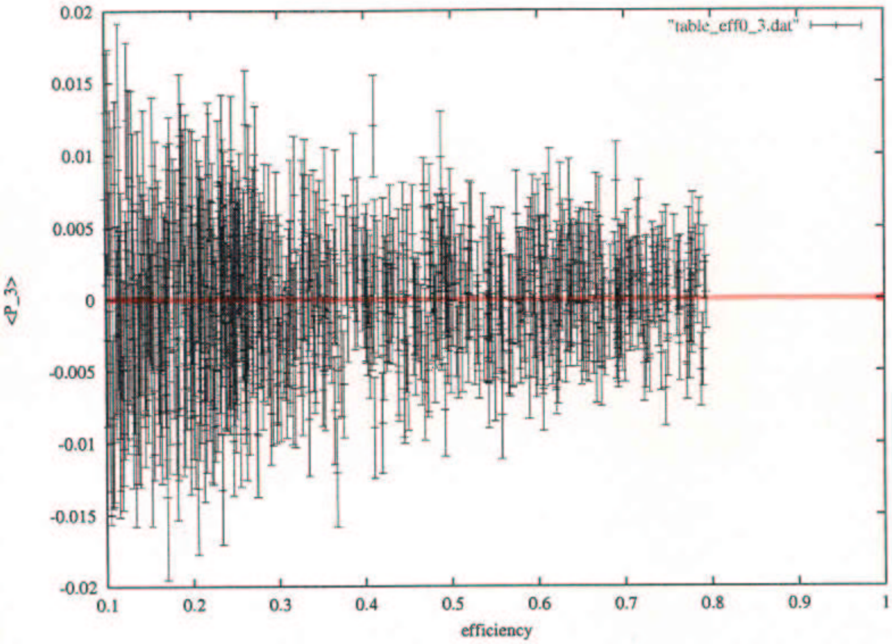

NO!

$\langle P_1 \rangle$

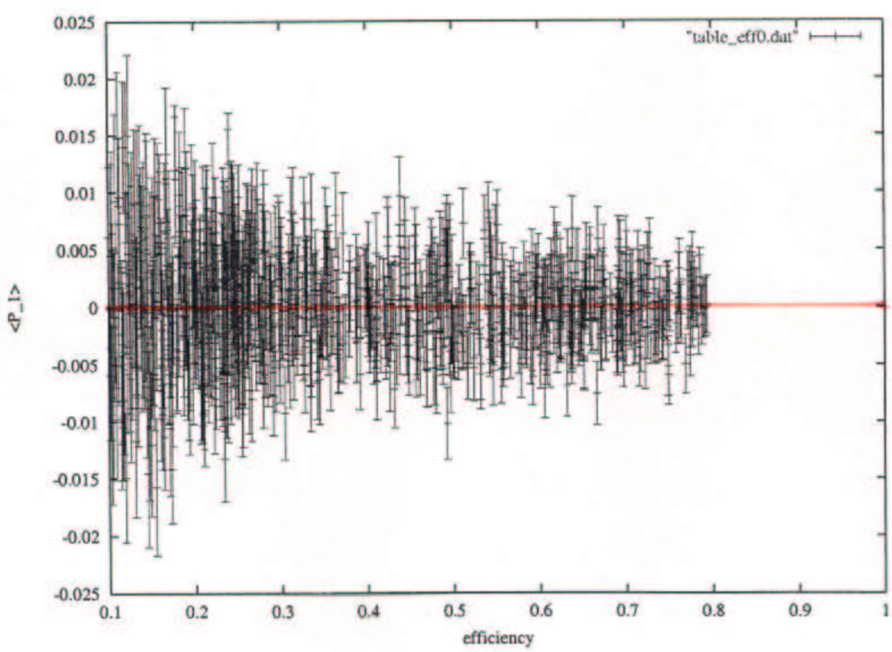

efficiency for $\pi^+\pi^-$ detection in HERMES

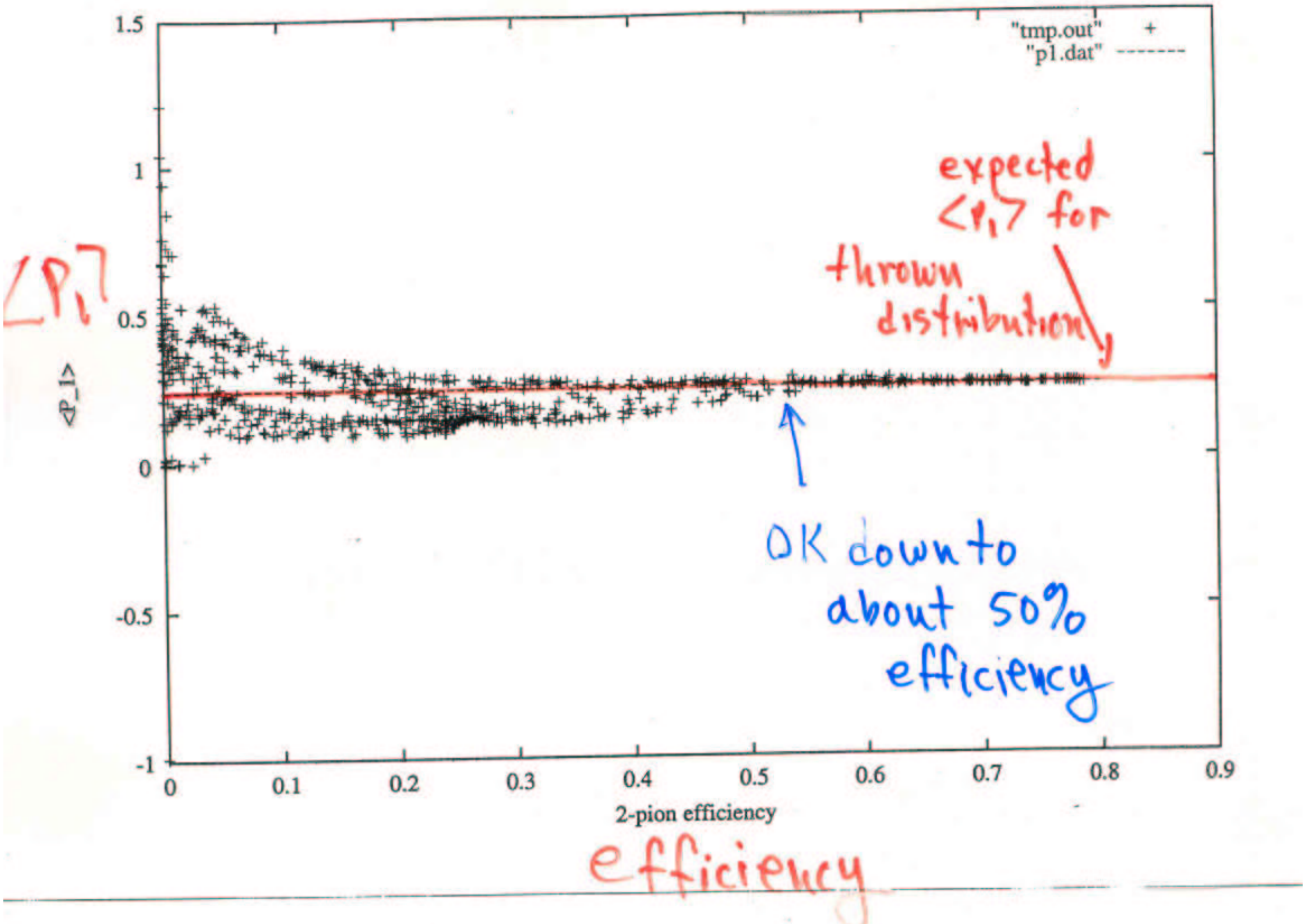
"tmp.out"
"p1.dat"
expected
<P1> for
thrown
distribution
OK down to
about 50%
efficiency
<P_1>
<P1>
2-pion efficiency
efficiency

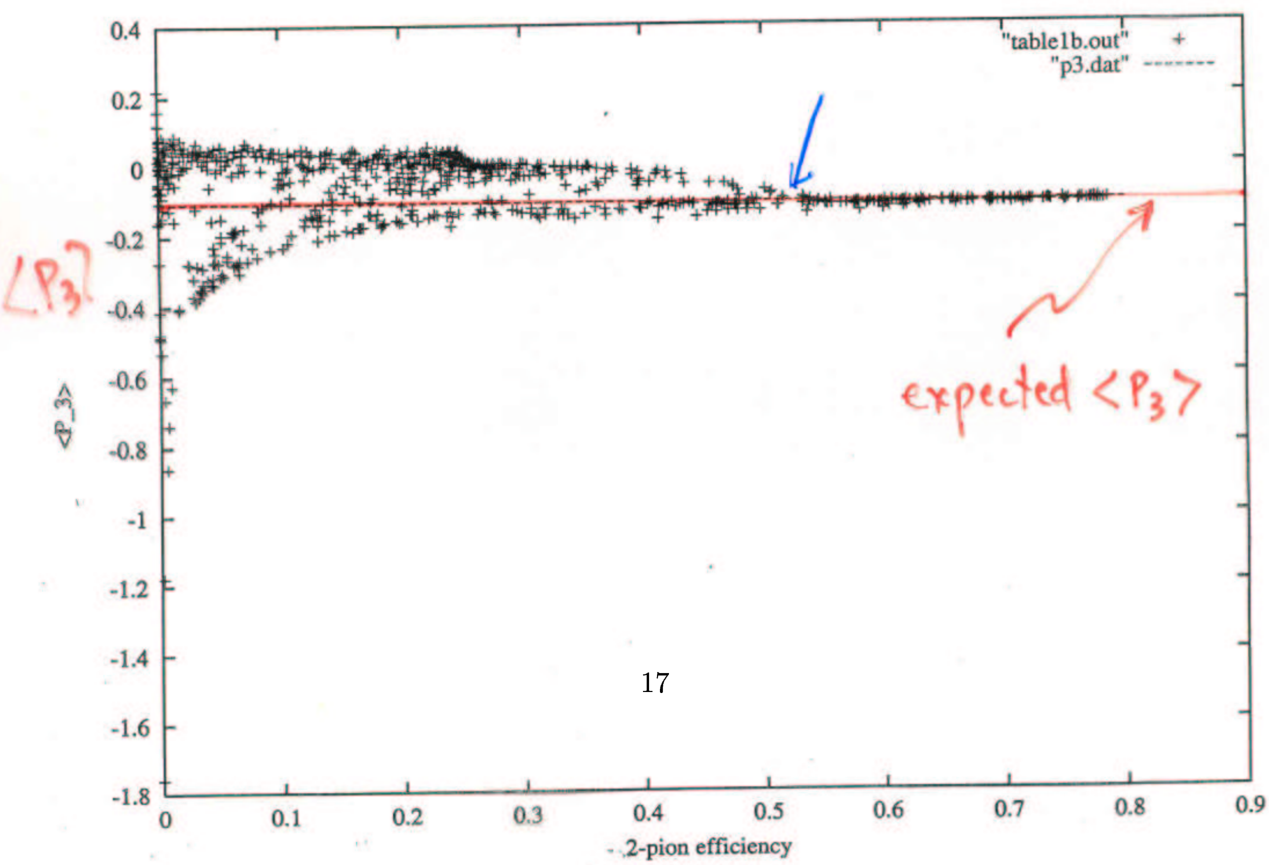
"table1b.out"
"p3.dat"
<P3>
<P_3>
expected <P3>
2-pion efficiency

MC

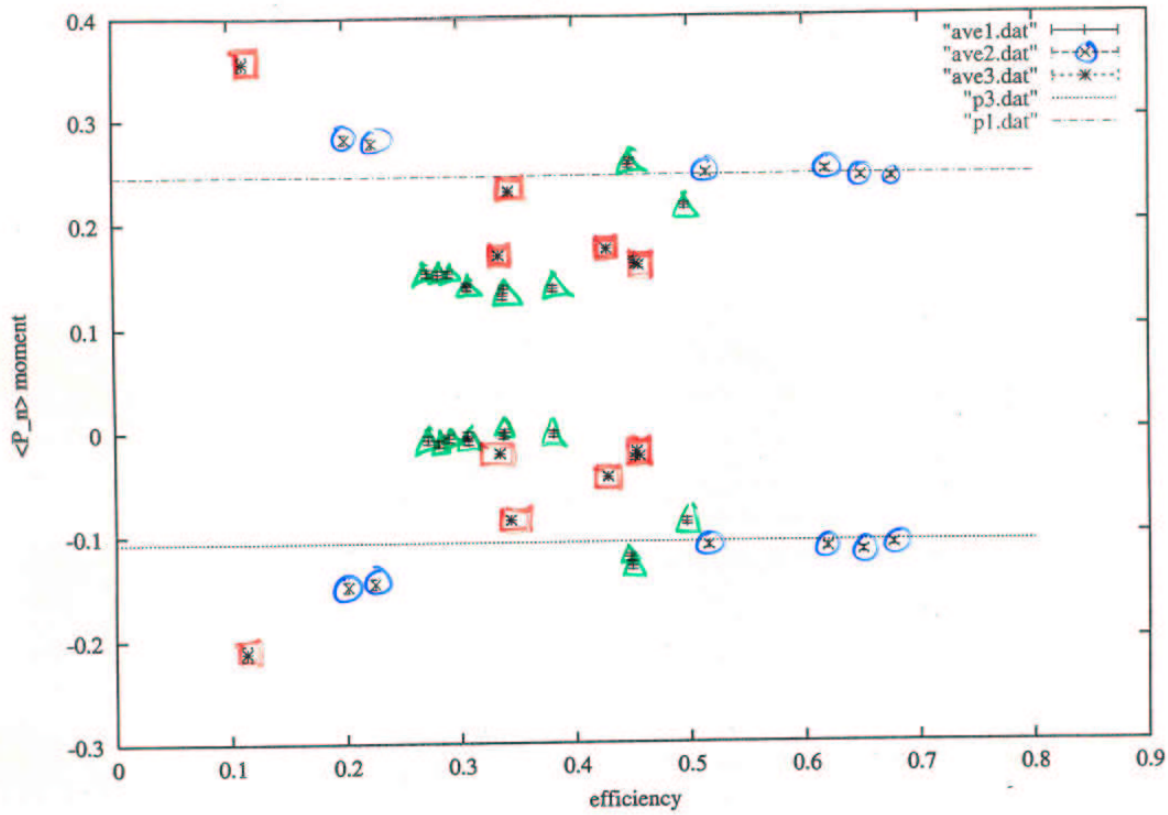

○ 6 bins in x for $0.3 < m_{\pi\pi} < 0.6$ GeV

□ 6 bins in x for $0.6 < m_{\pi\pi} < 0.95$ GeV

△ 11 bins in $m_{\pi\pi}$ for $x > .1$

INPUT $\langle x \rangle$ $\langle Q^2 \rangle$ $\langle m_{\pi\pi} \rangle$ for each bin
$\langle P_T \rangle$

In general, extracted $\langle P_n \rangle$ is far from expected value

Full averages over a bin will likely come closer to ideal value... but not completely.

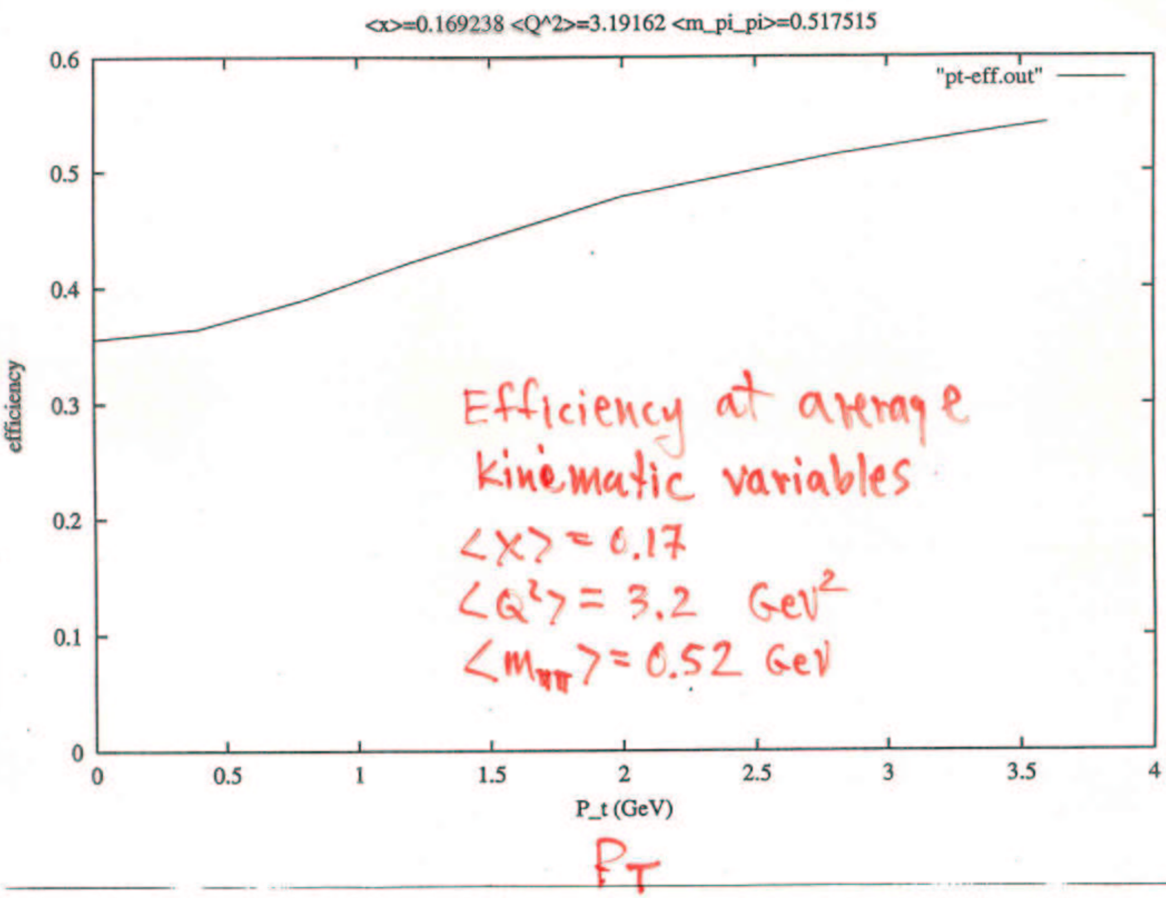

<x>=0.169238 <Q^2>=3.19162 <m_pi_pi>=0.517515
"pt-eff.out"
efficiency
P_t (GeV)
Efficiency at average kinematic variables
$\langle x \rangle = 0.17$
$\langle Q^2 \rangle = 3.2$ GeV^2
$\langle m_{\pi\pi} \rangle = 0.52$ GeV
P_T

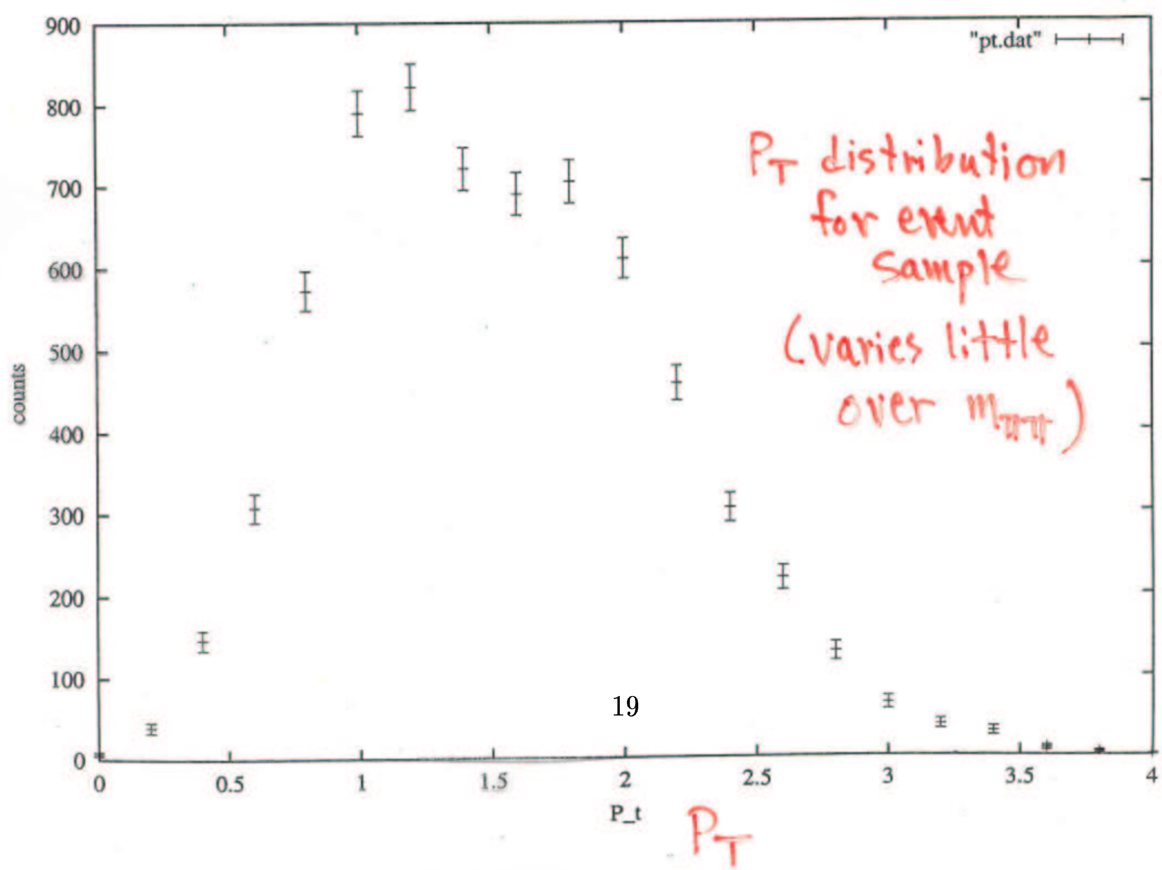

"pt.dat"
counts
P_t
P_T distribution for event sample (varies little over $m_{\pi\pi}$)
P_T

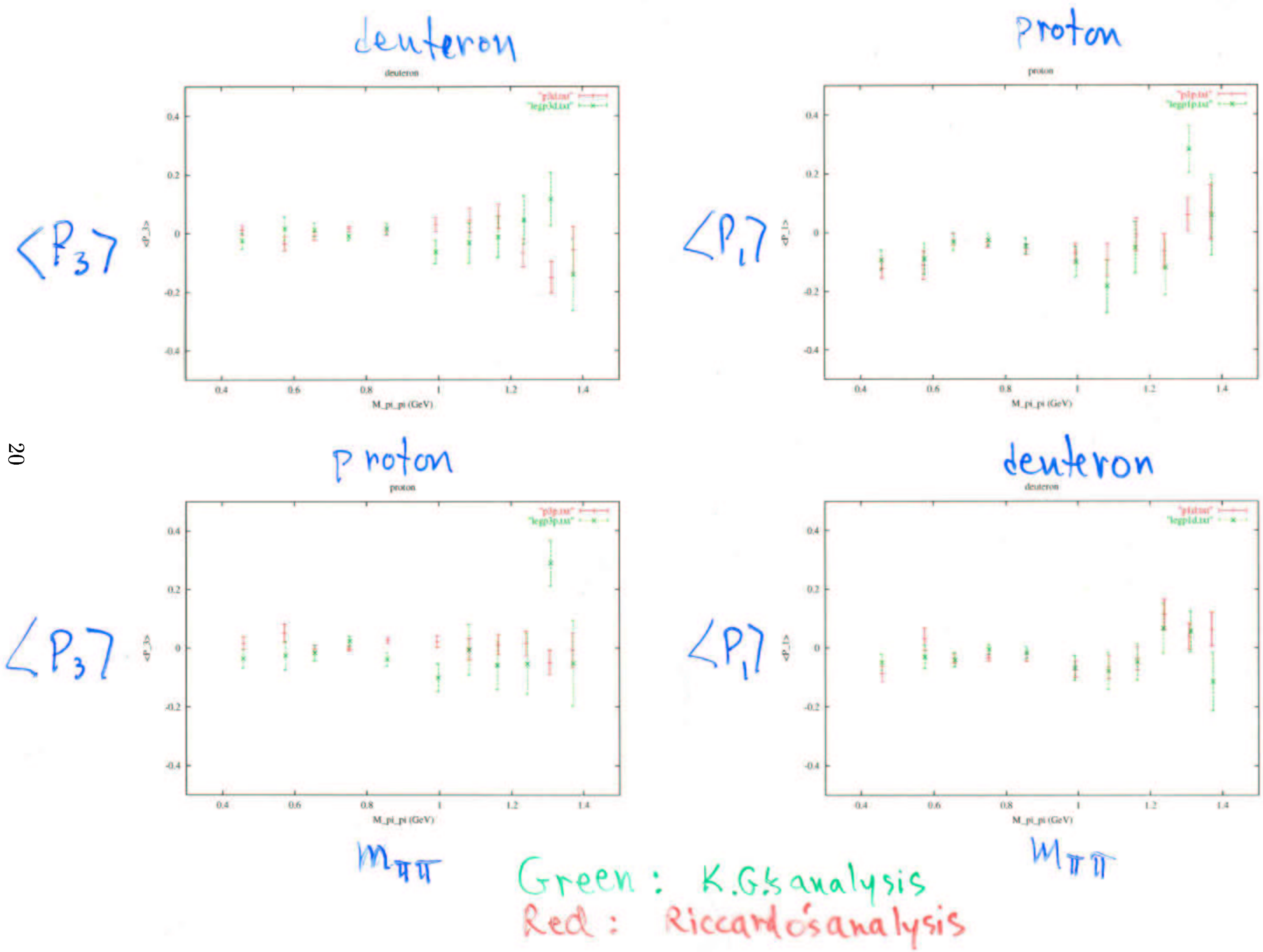
deuteron
deuteron
⟨P3⟩
<P_3>
M_pi_pi (GeV)
proton
proton
⟨P1⟩
<P_1>
M_pi_pi (GeV)
proton
proton
⟨P3⟩
<P_3>
M_pi_pi (GeV)
deuteron
deuteron
⟨P1⟩
<P_1>
M_pi_pi (GeV)
$m_{\pi\pi}$
$m_{\pi\pi}$
Green : K.G.'s analysis
Red : Riccardo's analysis

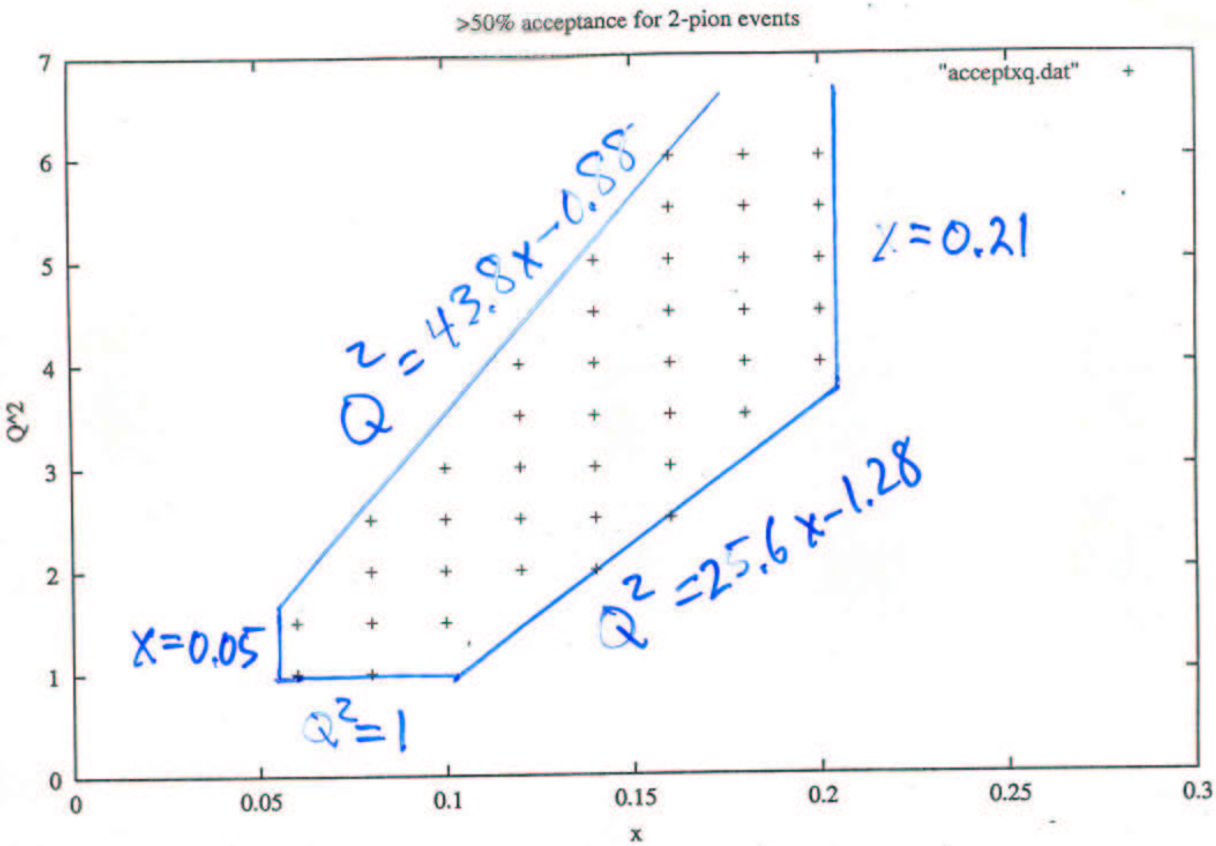

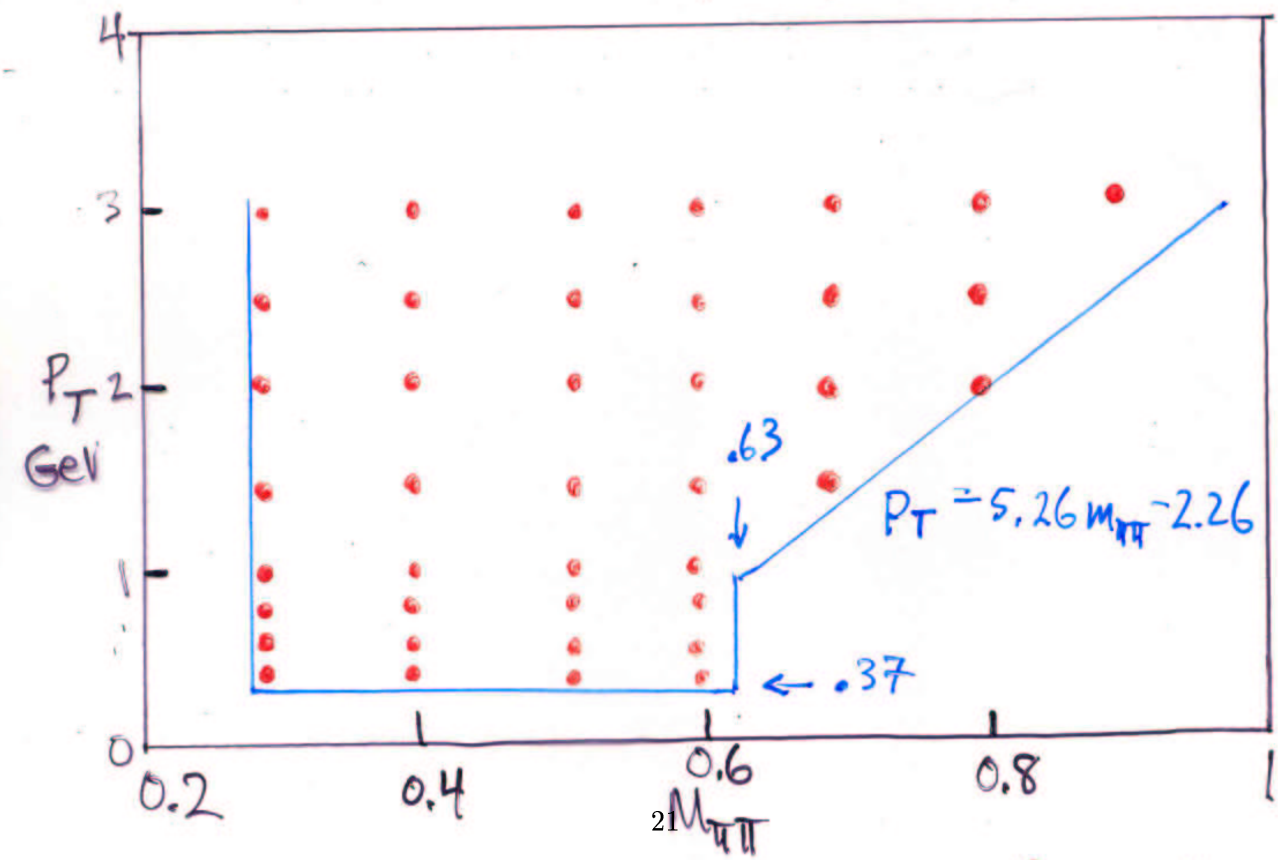

• population in bottom is the same for each point in the x-Q² plot

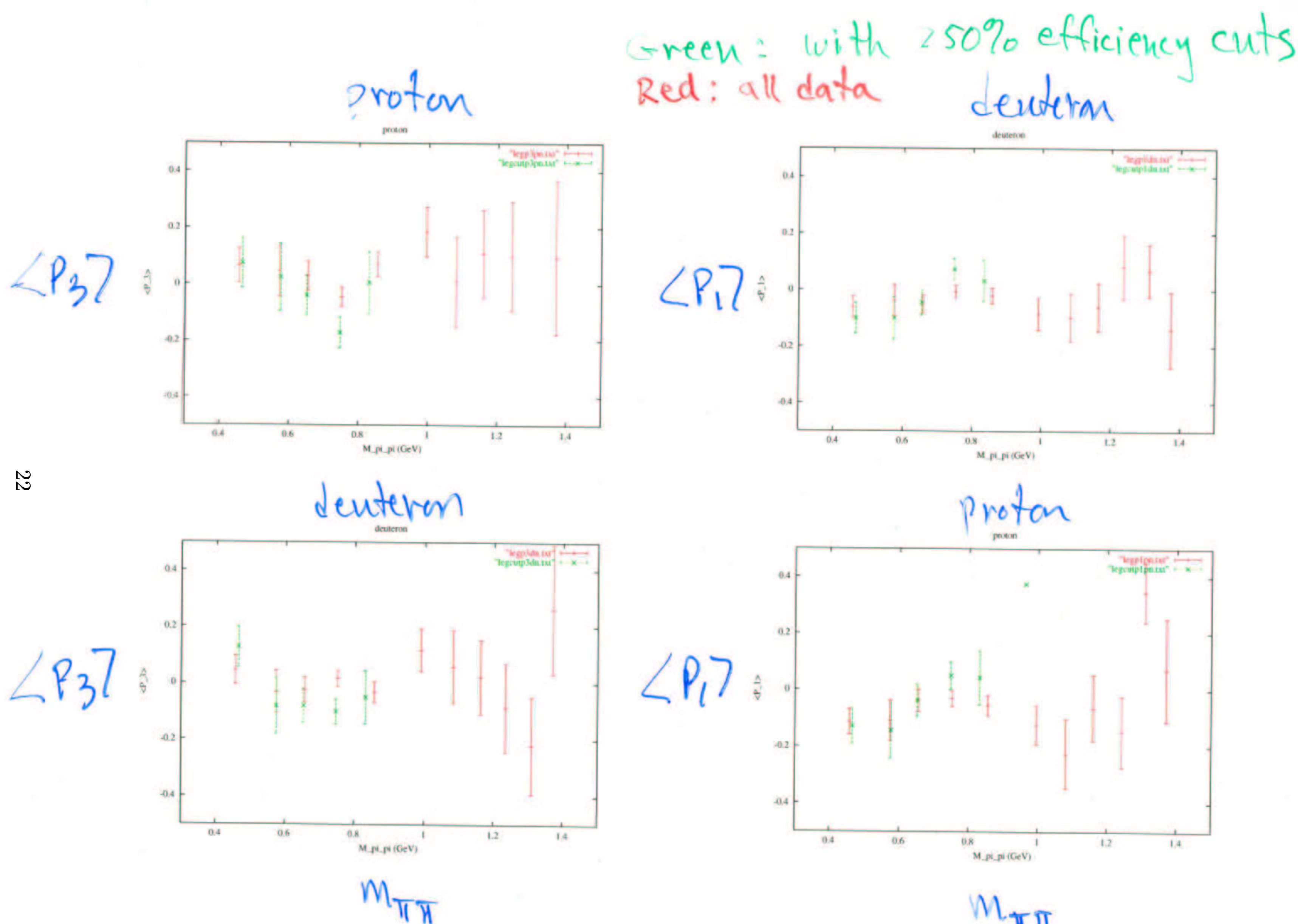
Green: with ≥50% efficiency cuts
Red: all data
proton
proton
"legp3pn.txt"
"legcutp3pn.txt"
$\langle P_3 \rangle$
<P_3>
M_pi_pi (GeV)
deuteron
deuteron
"legp1dn.txt"
"legcutp1dn.txt"
$\langle P_1 \rangle$
<P_1>
M_pi_pi (GeV)
deuteron
deuteron
"legp3dn.txt"
"legcutp3dn.txt"
$\langle P_3 \rangle$
<P_3>
M_pi_pi (GeV)
$M_{\pi\pi}$
proton
proton
"legp1pn.txt"
"legcutp1pn.txt"
$\langle P_1 \rangle$
<P_1>
M_pi_pi (GeV)
$M_{\pi\pi}$

deuteron

$\langle P_3 \rangle$

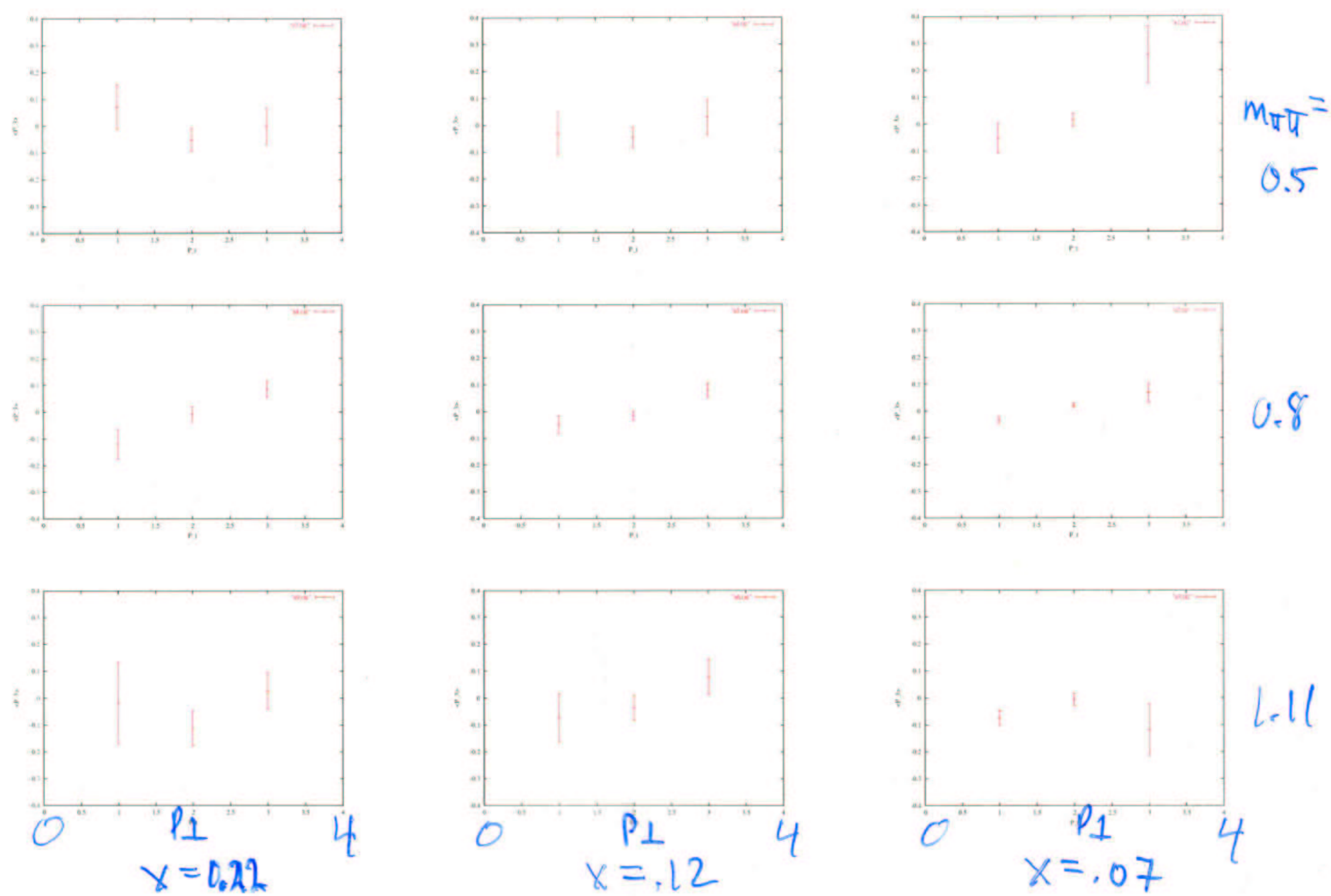

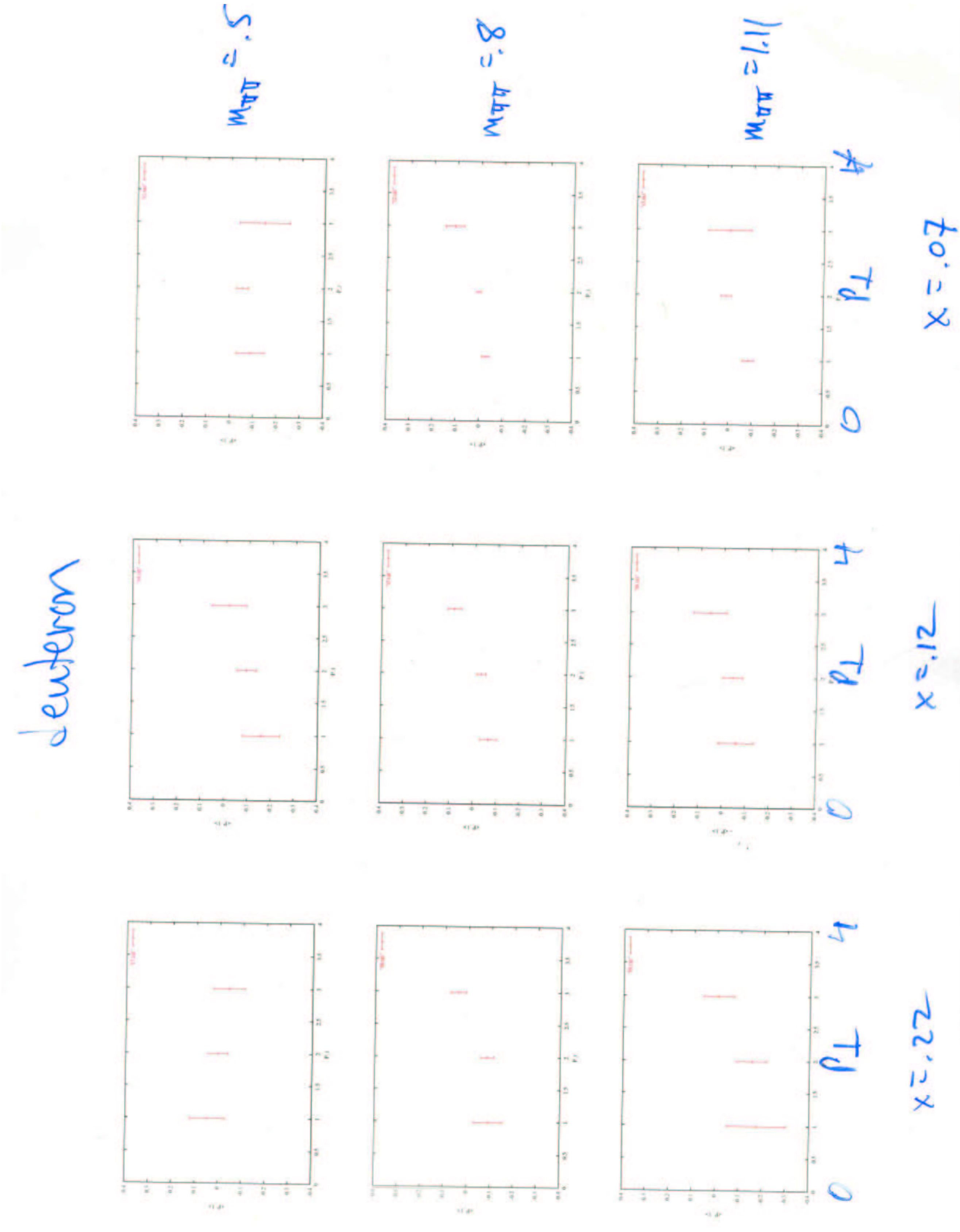
deuteron
x=.07
x=.12
x=.22
Td
0
4
$m_{\pi\pi}$=1.1
$m_{\pi\pi}$=.8
$m_{\pi\pi}$=.5

Conclusions

- Toy Monte Carlo is a nice way to get an understanding of $\langle P_n \rangle$ within HERMES acceptance

- Present estimations of errors in $\langle P_n \rangle$ due to acceptance are small compared to the statistical error bars.

$$\Downarrow$$

- Exclusive $\pi^+\pi^-$ analysis and paper are OK as they presently stand.

- Any future analysis with improved statistics will need to reckon with acceptance corrections to $\langle P_n \rangle$